

EVAPORITE VEINS OF SOUTHERN CALIFORNIA: SEARCHING FOR THE ORIGIN OF BORON AND LITHIUM IN CALCIUM SULFATE VEINS OF GALE CRATER, MARS D. Das¹, P. J. Gasda², R. J. Leveille¹, K. Berlo¹, M. A. Nellesen³, L. Crossey³, E. Peterson³, R. Beal³, A. L. Reyes-Newell², S. M. Clegg², A. M. Ollila², N. L. Lanza² ¹McGill University (debarati.das@mail.mcgill.ca); ²LANL; ³UNM.

Introduction: Boron and lithium are water-soluble elements that were detected within calcium-sulfate-filled fractures of Gale crater, Mars, using the Laser Induced Breakdown Spectroscopy (LIBS) instrument on board the ChemCam suite of the NASA *Curiosity* rover [1,2]. The Ca-sulfate veins in Gale crater containing B and Li also appear to show an inverse correlation [2]. In the clay-rich Murray formation, the enrichment of B in Ca-sulfate veins is attributed to remobilization of pre-existing evaporites [1]. However, the Ca-sulfate veins in Vera Rubin Ridge (VRR) indicate that B and Li may have been sourced out of surrounding clay-rich rocks after interaction with acidic fluids [2]. The inverse correlation of B and Li abundance in Ca-sulfate veins in VRR is attributed to a combination of dehydration, sequential precipitation, multiple generations of dilution and remobilization, and mixing with trace elements drawn out of clays during late-stage alteration [2]. Understanding the abundance and behavior of B and Li from a source to sink perspective that includes study of evaporites, clay-rich rocks and unaltered igneous rocks is key to gain insights on the late-stage diagenetic processes on Mars. Boron detection in Gale crater, is limited to low-Fe Ca-sulfates as Fe emission line interferes with the B emission line [1,2]. On Earth, clay minerals adsorb large amounts of B (>2000 ppm [3]) and Li (~5000 ppm [4]) and can play an important role in enrichment of diagenetic fluids. The study of terrestrial analogs can be useful as on Earth clays are lower in interfering Fe. Terrestrial analogs also enable a thorough approach for deconvoluting the geochemical signatures of alteration of primary rocks from mixed analyses.

In this study, we investigate a sample suite consisting of evaporites, clay-rich rocks, and igneous rocks from or near Death Valley (DV) in southern California as an analog to understand the alteration process in Gale crater. Gower Gulch is an important site for this study within DV because sulfates, borates, halites, basalts, and clay-rich rocks are reported together in the Furnace Creek area (Fig. 1) [5]. Although borates are not observed in Gale crater the presence of borates in an analog setting consisting of sulfates, halites and basalts (observed in Gale crater) is useful as it helps us understand the behavior of B in an evaporative setting. In DV, alternating evaporite-mudstone in the playa also shows evidence of interaction with groundwater and hydrothermal activity which incorporates processes that may be relevant for Gale crater [6]. The objective of this study is to identify the nature of interaction between evaporite diagenetic features and surrounding host rocks in DV, and discuss the implications for Gale

crater. This study will be especially valuable as *Curiosity* makes progress on the path up the sulfate unit and help understand more about the phases that we may encounter in Gale crater.

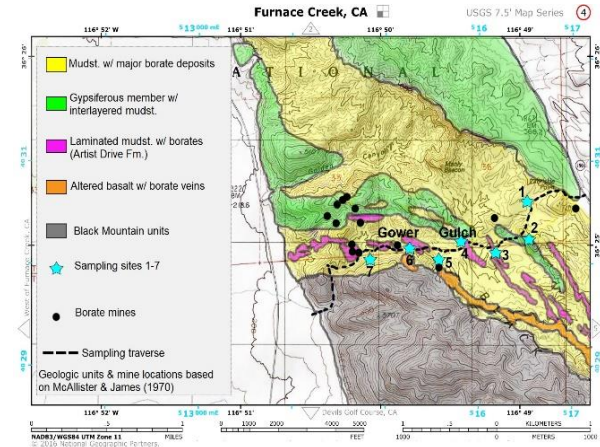


Figure 1. Geologic map of Furnace Creek, CA, indicating the geologic units and sampling sites in the Gower Gulch area. Geologic units, mine locations and elevations based on maps compiled by USGS [7,8].

Methodology: Sampling sites were chosen based on the presence of layered evaporite deposits such that we could collect vein samples cross-cutting multiple lithological layers: laminated mudstone (magenta) and gypsiferous members (green) next to altered basalts with borate veins (orange; Fig. 1 [7,8]) in addition to surrounding clay-rich bedrock samples. Gower Gulch in the Furnace Creek region, in Fig. 1 shows that borate and Ca sulfate deposits are close to each other [5]. Twenty one samples (Furnace Creek and Searles Valley) that are representative of both primary igneous rocks and weathered products (i.e., clay-rich rocks and evaporites) were selected for laboratory investigation at McGill University, Los Alamos National Laboratory (LANL), and University of New Mexico (UNM). This abstract will report the analytical results of these 21 samples analyzed using the ChemCam engineering unit at LANL [9] and X-Ray Diffraction instrument (XRD; UNM) using a Rigaku SmartLab Diffractometer with a 5° source and detector Soller slits. Data was collected at 6°/min with a 0.02° step size with a collection range of 3-150° 2θ. Copper is used for the X-ray source.

Results: An A-FM-CNK diagram for the DV samples analyzed and the mineralogy for each sample identified using XRD along with reference DV pluton and illite samples shows mixing between unaltered samples and weathering products (Fig. 2A) [11]. The relationship between the DV and reference samples on a CaO (mobile)

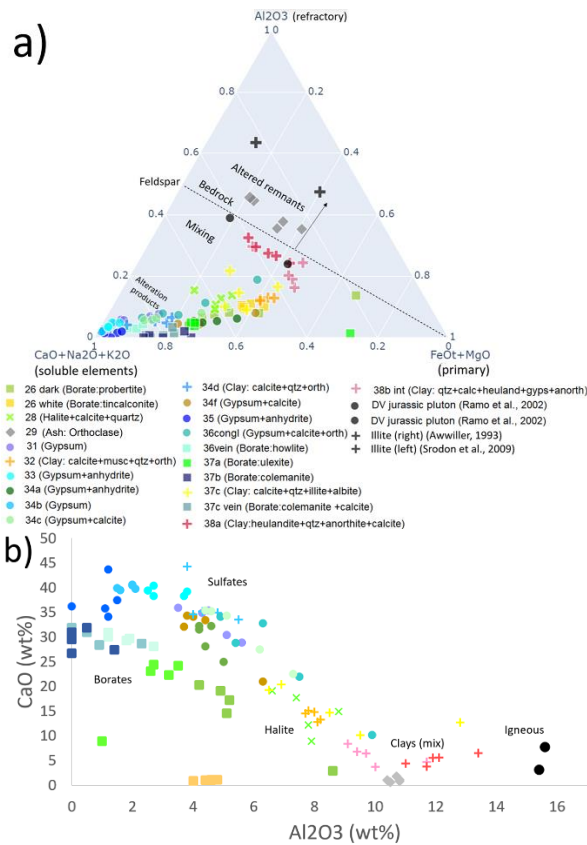


Figure 2. A) A-FM-CNK ternary plot (mol%) of rock samples from DV with respect to previously reported igneous rocks and illite standards [11]. Sulfates-rich rocks are indicated by filled circles, borate-rich rocks by squares, clay rich samples by cross, halite-rich rocks by X, and orthoclase-rich ash by filled diamond. B) Immobile (Al_2O_3) versus mobile (CaO) element scatter plot.

vs Al_2O_3 (immobile) scatter plot also show a similar mixing trend (Fig 2B). Some evaporite samples also show the presence of Cr and F as indicated by relative higher-intensity peaks in the LIBS data (Fig 3A and B).

Discussion: Fig 2A indicates mixing between varying amounts of aluminous clays, soluble/mobile elements, and unaltered materials. Upon weathering, igneous rocks lose water soluble mobile phases ($CaO+Na_2O+K_2O$) and become relatively Al_2O_3 (i.e., clay) rich and move upwards towards the $FeO_T+MgO-Al_2O_3$ join [10] (arrow; Fig 2A). Our 21 samples and 4 reference samples (igneous and illite rocks) [11-13] indicate where Ca-free clay rich rocks would fall on the diagram. This figure shows that the evaporites fall close to the CNK apex, while the clay-rich samples fall between the evaporites and DV igneous samples near the feldspar line. Pure illites fall closer to Al_2O_3 compared to the DV rock samples indicating that the DV clay-rich samples are pulled towards the CNK apex due to the presence of

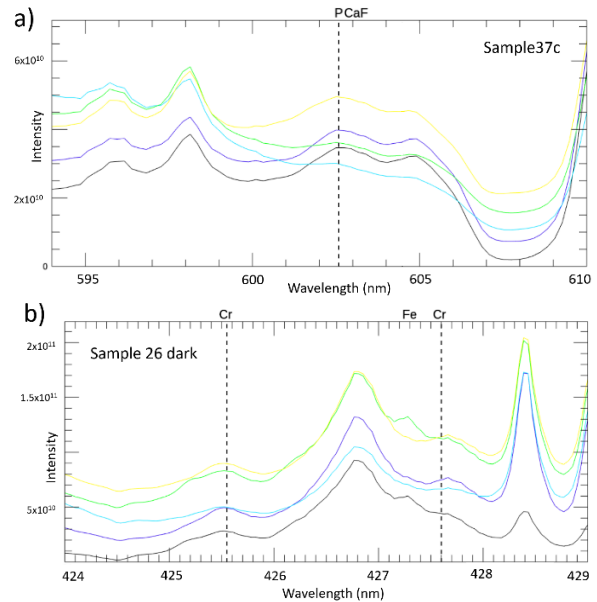


Figure 3. A) LIBS spectra showing the potential presence of CaF in clay-rich sample 37 c. B) LIBS spectra showing the presence of Cr in borate-rich sample 26 dark.

evaporites. A similar mixing trend is observed in Fig 2B, and borates and sulfates fall in two different clusters in this plot.

Hydrothermal processes on Earth produce Cr-rich serpentinization products and F enrichment [14,15]. The presence of Cr and F in the samples likely represent a hydrothermal influence in in evaporites of DV [6]. This makes the sample suite relevant to Gale crater as hydrothermal activity is suggested by [16].

Conclusions and Future Work: Clay rich rocks of DV show mixture with evaporites and possible hydrothermal signatures. The sample set collected from southern CA enables us to study the behavior of water soluble elements observed in Gale crater from a source to sink perspective. Next steps in this project will aim to deconvolute chemical weathering and mixing geochemical trends using FULLPAT XRD analysis to understand how elements partition in mineral phases within each sample. We also aim to analyze minor elements such as Cr and F to understand possible hydrothermal influence. Principal component analyses on LIBS data will be done to constrain sample groups.

Acknowledgements: NSERC Discovery program, CSA support for NASA MSL Participating Scientists, NASA Mars Exploration program. **References:** [1] Gasda et al. (2017) *GRL* 44(17), [2] Das et al. (2020) *JGR:P*, [3] Nellessen et al. (2021) *LPI*, 2694, [4] Vine and Dooley (1980) USGS, [5] Swihart et al. (2014) *Econ. Geol.* 109(3), [6] Tanner (2002) *Sed. Geol.*, 148(1-2), [7] McAllister et al. (1970) *Geol. of FC Borate Area, DV(14)*, [8] USGS (1952) *1:62500-scale Quad:Furnace Creek*, [9] Clegg et al. (2017) *SCA* 129(64-85), [10] Hurowitz and McLennan (2007) *EPSL* 260(3-4), [11] Rämö et al., (2002) *CMP* 143(4), [12] Awwiller (1993) *JSR* 3(501-512), [13] Środoń et al., (2009) *CCM* 5 (649-671), [14] Hodel et al., (2017) *PR* 300 (151-167), [15] Worden et al., (2018) *Springer* (185-260), [16] Gasda et al., (2021) *LPI* 2548.